JURNAL SAINS MATERI INDONESIA (JUSAMI)
ISSN: 1411-1098 (print), 2614-087X (online)
VOL. 25, ISSUE 2, 2024
DOI:10.55981/jsmi.2024.893

ORIGINAL ARTICLE

Effect of Precursor Solvent on the Carbon Micro-Structures Derived from Spray Pyrolysis of Pine Resin (Gondorukem): Preliminary Study

Jayadi[1], W. B. Widayatno[2], A. S. Wismogroho[2], C. Firdharini[2], A. Maddu[1] and Y. W. Sari[1*]

[1]Biophysics Graduate School IPB University, Indonesia
[2]Research Centre of Advanced Material, The National Research and Innovation Agency of Indonesia, Indonesia

ABSTRACT – Carbon materials have been widely used in various fields. This study aimed to produce carbon using spray pyrolysis with pine resin (gondorukem) as the precursor and different solvents, namely gondorukem-acetone (GAC), gondorukem-ethyl acetate (GEA), and gondorukem-dichloromethane (GDC). The precursor was prepared in a 1:8 (m/v) ratio, and the spray pyrolysis method was employed by heating the atomized precursor solution in the heating zone of a tube furnace. The atomization precursor was infused with nitrogen gas at a rate of 1 l/min with furnace temperature set at 1000°C with heating times of 5, 10, and 20 mins. The carbonaceous materials produced from the pyrolysis were collected on the wire mesh 1000 that was put on a stainless pipe. Carbon that has been coated on the wire mesh 1000 was analyzed using the optical microscope (OM). The physical properties and morphology of the synthesized carbonaceous material were analyzed using field emission scanning electron microscopy (FE-SEM), Fourier-transform infrared spectroscopy (FTIR), Raman, and Brunaur-Emmett-Teller (BET). Based on FE-SEM analysis, the particle size of the GAC sample has an average of 283.58 nm and the highest carbon content, which reached an average of 97.312 At%. GAC samples had the lowest disorder properties in the Raman spectroscopy test, with the value of ID/IG reaching 0.795764. The functional groups observed were C–H stretching at 2920.49 cm^{-1}, N–H bending at 1629.07 cm^{-1}, and C–O stretching at 1159.70 cm-1. Based on carbon content, disorder properties, and functional group stabilization, carbon from the GAC precursor provides the ideal characteristics to be used as a filter material in medical masks. Meanwhile, based on BET testing, the carbon materials from GEA have the ideal material morphological properties to be used as a filter in medical masks. Spray pyrolysis is an efficient method for producing carbon materials, and the use of gondorukem as the precursor shows great potential for various applications.

ARTICLE HISTORY
Received: 4 Jul 2023
Revised: 29 Sep 2023
Accepted: 02 Okt 2023

KEYWORDS
Carbon
Microstructures
Pine resin (gondorukem)
Spray Pyrolysis

INTRODUCTION

Carbon-based material is well-known for its versatile morphology, size, and reactivity, which lead to excellent physical and chemical properties [1]. Carbon-based material can also be utilized for various applications such as membrane and water waste processing [2], biosensors [3], battery [4], filler on polymer composite [5], fuel cell catalyst [6], electronics [7], energy storage [8], and even for medical sciences [9]. The structural properties of carbon, such as their morphology, particle size, porosity, and specific surface area, are mainly determined by the synthesis methods and conditions [8]. Researchers have investigated using top-down approaches such as chemical oxidation, electrochemical oxidation, ultrasonic methods [10], [11], solvent extraction [12], a hydrothermal method [13]–[15], solvothermal [16], high-pressure high-temperature [17], and spray pyrolysis [18]. However, most of these methods are known to require expensive materials, tough synthesis conditions [11], [19], lengthy reaction times, the use of catalysts, and specific conditions, so it is considered to be inefficient [20]. Spray pyrolysis is an efficient method that has been observed to synthesize carbon material with great promise in the recent past [21].

Spray pyrolysis is the method of producing carbon by heating the atomized of precursor solution. It is a generic process for producing particles by decomposing precursor molecules at high temperatures [22]. Spray Pyrolysis also known for its conversion of smaller carbon structure to the desired size [11]. A typical spray pyrolysis system is composed of a reservoir for precursor solution, droplet generator, reactor, and collection unit. Precursor solutions of aqueous or non-aqueous solvents are atomized and carried by a gas into a reactor where droplets are evaporated and decomposed into solid particles [23]. Electrical heating or flame provides heat for evaporation of solvent and decomposition of precursor. Some non-conventional heating methods, such as microwave or laser, are employed for controlling morphology. The heating temperature of the reactor also determines the physical properties of the carbon produced. Carbon nanotube (CNT) arrays were synthesized by employing spray pyrolysis using ferrocene and xylene solution as liquid precursors [24]. It was found that nanomaterials were grown only in the synthesis temperature range of 700–800°C. A maximum CNT length of 63 μm was obtained at 800°C. Additionally, the diameter of CNTs decreased dramatically from 54 to 19 nm as the temperature was increased from 700–800°C [9]–[10]. This proves that the temperature in the synthesis process can affect

*CORRESPONDING AUTHOR | Y. W. Sari | ✉ yessie.sari@apps.ipb.ac.id

the growth process of nanomaterials itself. Furthermore, the composition and type of solvent used in the precursor affect the physical and morphological properties of the carbon material produced. Darabont et al. [25] used spray pyrolysis to synthesize carbon nanotubes from a precursor of benzene (n-pentane, n-hexane, n-heptane, and n-octane) mixed with ferrocene. According to the results of this work, the precursor 3 g ferrocene/50 ml n-heptane benzene produced the most carbon material, reaching 1.44 g with a purity approaching 70%. The nanotubes of the sample are mostly straight, and their surface is smooth also covered with amorphous carbon [25].

Several carbon-based solvents, including methane, acetylene, benzene, xylene, and toluene, have been utilized as raw materials to produce carbon microstructures and carbon nanotubes [26]. These precursors are generated from fossil fuels, which will be exhausted in the future. Besides, carbon was successfully produced from acetone, ethyl acetate, and dichloromethane with 45.1% [27], 86.4% [28], and 13% [29] yield, respectively. The carbon structures produced from acetone, ethyl acetate, and dichloromethane differ. Carbon synthesized using acetone and ethyl acetate forms carbon nanotubes [27], [28] while carbon synthesized from dichloromethane forms porous carbon [29]. This encourages the exploration of alternative precursors in the synthesis of carbon, including turpentine oil [12]–[13] as a precursor. Turpentine oil is a natural combination of turpentine obtained from the distillation of resin extracted from pine trees [30]. Turpentine oil and gondorukem are refining materials made by steam distillation of pine tree liquid (oleoresin). Gondorukem has a solid form which is brownish-yellow in color. Indonesia is a country that produces gondorukem on a large scale, with total exports of 67,162 tons in 2018 [31]. That was supplied by eight companies with a total capacity of 92,550 tons. With this massive production, gondorukem may serve as a potential precursor for the synthesis of carbon microstructures.

In this study, the effect of the solvent type used for the synthesis of carbon microstructures using the spray pyrolysis method is investigated. The precursor is prepared from pine resin (gondorukem) mixed with a solvent. Acetone, ethyl acetate, and dichloromethane are the three solvents used. Experiments will be conducted with various synthesis times. Based on the optical microscope (OM) analysis and the amount of carbon created, the optimum synthesis time will be utilized as a reference for research investigation in determining the physical properties and morphology of the carbon microstructures synthesized, which will be analyzed based on the field emission scanning electron microscopy (FE-SEM), Fourier-transform infrared spectroscopy (FTIR), Raman, and Brunaur-Emmett-Teller (BET) tests.

EXPERIMENTAL METHOD

Experimental Procedure

The carbon microstructure is synthesized by dissolving the precursor of pine resin (gondorukem) in various solvents. Acetone (GAC), ethyl acetate (GEA), and dichloromethane (GDC) were used as solvents. Pine resin (gondorukem) was mashed to reach a size of 60 mesh. The solvent, which is acetone, has a purity of 99.75% produced by Mallinckrodt Chemicals, as well as ethyl acetate and dichloromethane have a purity of 99.8% produced by Merck KGaA.

The precursor was prepared in a 1:8 (m/v) ratio. This research was made using 25 grams of gondorukem mixed with 200 ml of solvent. The effect of the gondorukem-to-solvent ratio was investigated with variations of 1:4, 1:8, and 1:16. The ratio of precursors should influence the physical characteristics of the synthesized carbon. Spray pyrolysis was infused with nitrogen gas at a rate of 1 l/min, and the furnace temperature was set at 1000 °C with heating times of 5, 10, and 20 mins for each precursor with different solvents. The carbon will be produced during the heating process of the atomized precursor. It will be collected on the wire mesh 1000 put on a stainless pipe.

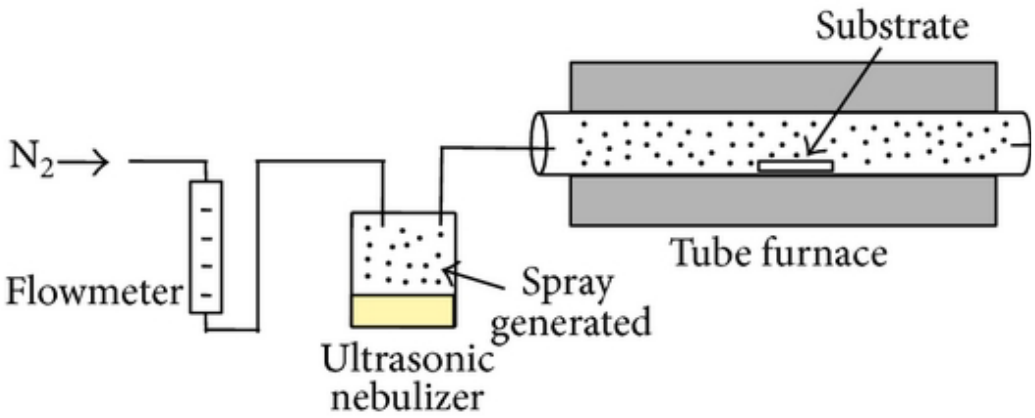

Figure 1. Illustration of spray pyrolysis system [32] with modification, where substrate collected in a wiremesh

Tests and Measurements

Carbon that has been coated on the wire mesh 1000 will be analyzed by optical microscope (OM) test using the VHX-5000 digital microscope with super high-resolution imaging mode that uses short-wavelength light and pixel shift

technology to improve resolution by up to 25% with a magnification range from 0.1–5000 times. On the other hand, the physical properties and morphology of the carbon material, which will be analyzed by the field emission scanning electron microscopy (FE-SEM) test using JIB-4610F, enables high-resolution SEM observation and high-speed analysis with a variety of analytical instruments, such as energy-dispersive X-ray spectroscopy (EDS) to perform crystallographic characterization. The Fiji ImageJ application was used to analyze the particle size in the FE-SEM test results [33]. The acquired particle size is the mean of 20 carbon particles measured using the application with scale calibration on the order of nanometer (nm). The Fourier-transform infrared spectroscopy (FTIR) test to determine the functional group will be carried out using Fourier-transform infrared spectrometer from Thermoscientific Nicolet iS-10 that is complete by infrared spectroscopy system with a wavenumber range from 400–7500 cm^{-1}. Raman spectroscopy will be carried out using Horiba 550 with laser wavelength of 532 nm, grating 1800 g/mm, and spectral range from 200–3000 cm^{-1}. Brunaur-Emmett-Teller (BET) surface area and pore size analysis will be done using Quantachrome Nova 4200e, which produces BET surface area as well as pore size and is capable of measuring both adsorption and desorption isotherms in a few hours. The surface area range starts from 0.01 m2/g, and the pore size range is 0.35–400 nm.

RESULTS AND DISCUSSION

The pyrolysis conducted in this study decomposed the carbonaceous materials of gondorukem. The use of different types of solvents would result in different decomposition processes. After passing through a heating reactor during the spray pyrolysis process, the synthesis of microstructure carbon using a precursor mixture of gondorukem with acetone (GAC) and gondorukem with ethyl acetate (GEA) produced brownish smoke. This may relate to the heating process that decomposes the precursor in the heating area of the reactor (furnace). In contrast, the precursor mixture of gondorukem and dichloromethane (GDC) produced thick black smoke during the synthesis process. The production of this thick black smoke may relate to the GDC precursor that contains chlorine (Cl), which decomposes more easily during the heating process. GDC also has a lower evaporation point than other precursors. Following the spray pyrolysis, the carbon nanomaterials produced were collected using wire mesh 1000. The presence of carbon powder coating the wire mesh 1000 was further evaluated using an optical microscope (OM). It was trimmed to 10×10 mm size and then prepared on a microscope slide to provide the wire mesh with a flat surface.

Morphology Evaluation

The morphology of carbon was determined by optical microscope and field emission scanning electron microscopy (FE-SEM). The optical microscopy (OM) was carried out on 1000 wire mesh sheets, both uncoated (Figure 1) and coated with carbon materials, resulted from spray pyrolysis of gondorukem with three different types of precursors GAC, GEA, and GDC (Figure 2). The test was performed at several magnifications. Figure 3 (a), Figure 3 (b), Figure 3 (c), Figure 3 (d), Figure 3 (e), and Figure 3 (f) show pictures of the results of the OM test at 500 times magnification with time variations of 5, 10, and 20 minutes.

Figure 2. Image of wire mesh 1000 without carbon coating by OM test (500× magnification)

According to the OM test results in Figure 3 (a), Figure 3 (b), and Figure 3 (c), the increase in synthesis duration time would reduce the porosity of the wire mesh coated by carbon materials obtained from GAC and GEA precursors. This means that more carbon particles have collected on the surface of the mesh. However, a different phenomenon occurred once the mesh was coated with carbon materials resulting from GDC (Figure 3 (g) and Figure 3 (h)). In this mesh, the wire mesh was damaged. This might be due to the fact that the GDC precursor contains the element chlorine (Cl), which will react with the wire mesh in the atmosphere or cause corrosion to grow on the wire mesh surface.

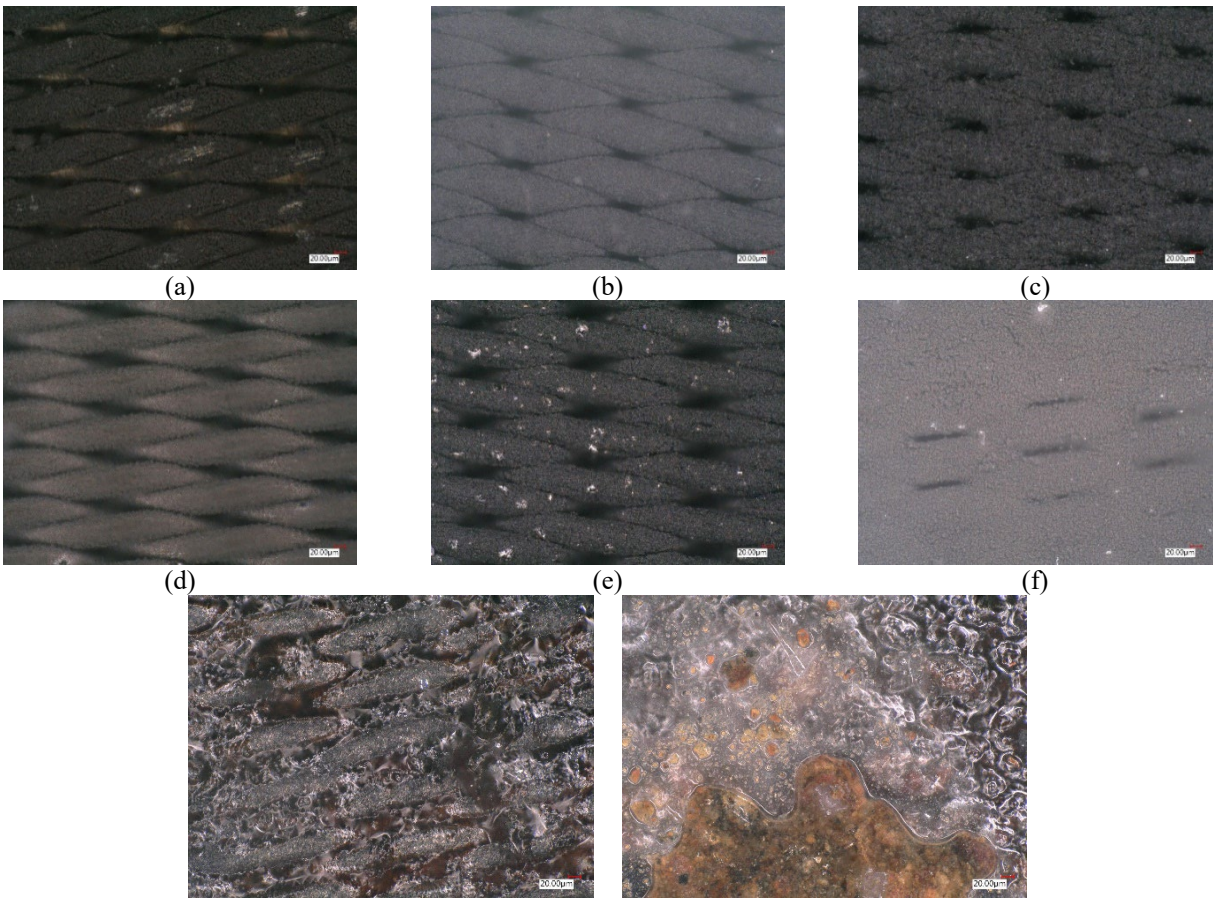

Figure 3. Image of wire mesh 1000 by OM test (500× magnification) for precursor GAC (a) 5 minutes, (b) 10 minutes, and (c) 20 minutes; for precursor GEA (d) 5 minutes, (e) 10 minutes, and (f) 20 minutes; for precursor GDC (g) 5 minutes and (h) 20 minutes

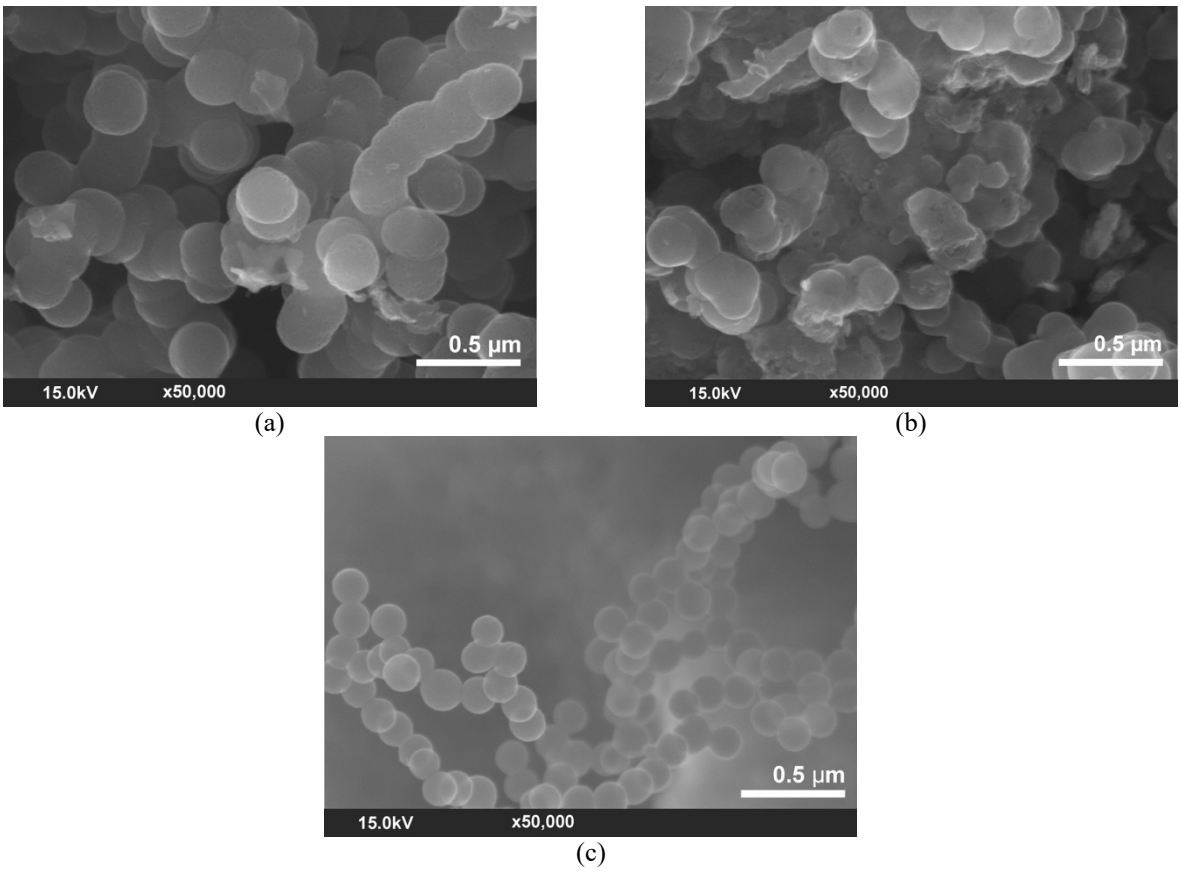

Figure 4. FE-SEM image of carbon that synthesized from precursor (a) GAC, (b) GEA, and (c) GDC in 20 minutes

The FE-SEM analysis determines the particle picture of the test material at high magnification. The FE-SEM test may be used to observe the form and size of the particles qualitatively, as well as to determine the content at various spectrum points. The FE-SEM analysis was conducted at carbon powder of GAC, GEA, and GDC samples obtained from spray pyrolysis for 20 minutes (Figure 3 (a), Figure 3 (b), and Figure 3 (c)).

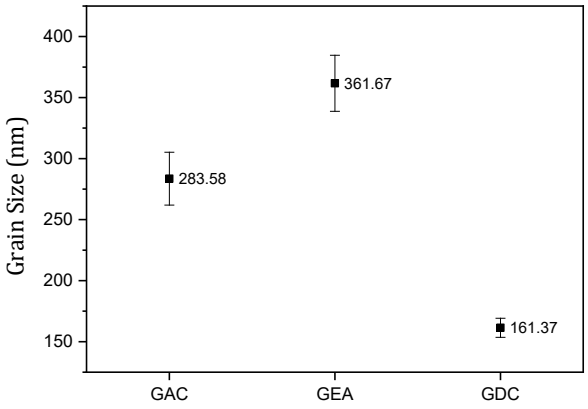

Figure 5. Size of the grains deposited on carbon wire by Fiji ImageJ

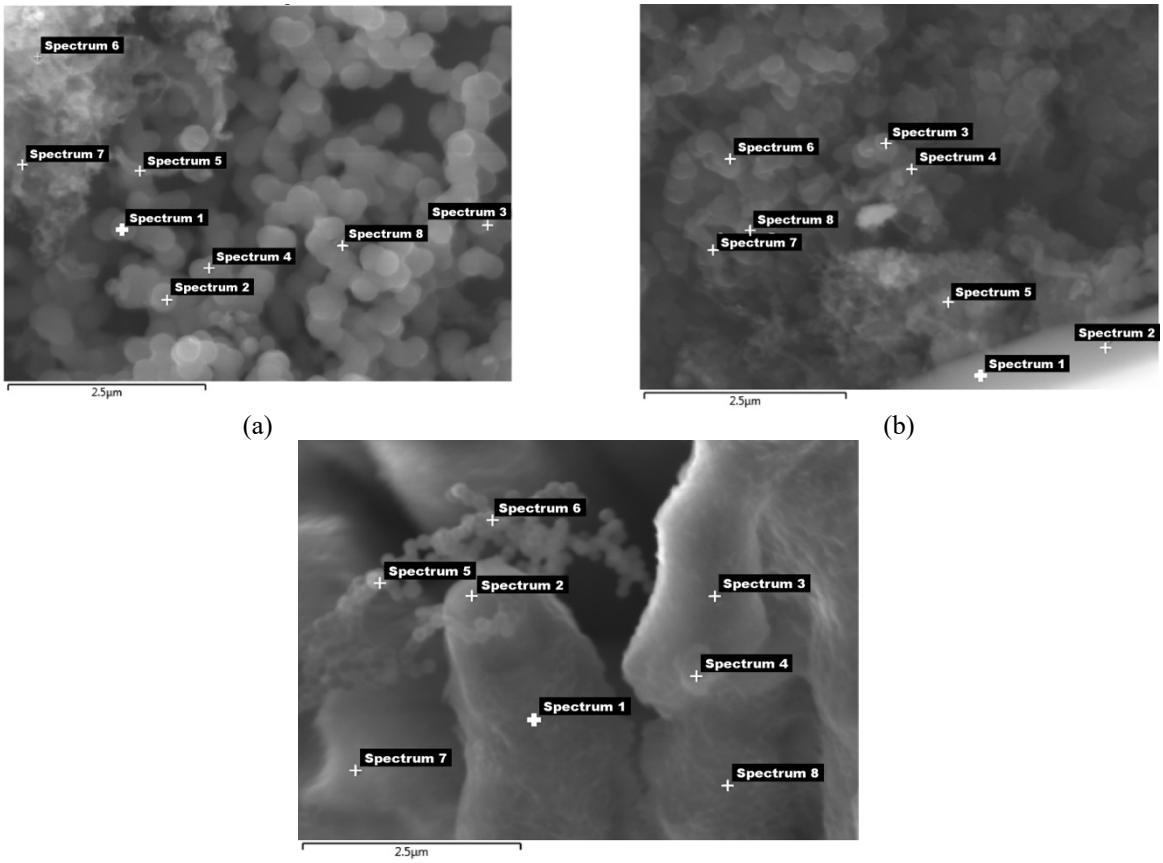

Figure 6. Spectrum point analysis of carbon from precursor (a) GAC, (b) GEA, and (c) GDC

According to the FE-SEM results, the grain has a relatively round shape (Figure 4 (a), Figure 4 (b), and Figure 4 (c)) and size in the order of nanometer (Figure 5). The average size of 20 carbon particles was used to estimate the carbon particle size based on the findings of the ImageJ application analysis (Figure 5). According to this analysis, the smallest average carbon particle size comes from the GDC precursor, with a value of 161.37 nm and the lowest error value. The carbon particles from the GAC precursor have an average size of 283.58 nm, while the carbon particles from the GEA precursor get the largest average size, reaching 361.67 nm. Elemental content analysis was also performed at several points in this test (Figure 6). Each sample has eight test spectrum points. The carbon synthesized with GAC precursors is not the exact percentage of the carbon but relatively had the highest percentage of carbon (C), reaching an average of 97.3 %. Meanwhile, the GEA precursor has a carbon element percentage value of 83.6%, and the GDC precursor has the lowest value, which is 61.3%, as shown in Table 1. Micro-structured material is one that has an internal or external structure composed of interconnected constituent elements in the nanoscale range. The nanoscale has a size range of

around 1 to 1000 nm [34]. So, based on that definition, carbon material produced from GAC, GEA, and GDC precursors by spray pyrolysis in this study includes microstructure material [34].

Table 1. Shows At% carbon from FE-SEM test

Spectrum Point	Relative Carbon Content (Wt%)		
	GAC	GEA	GDC
1	97.6	62.3	62.3
2	97.6	61.5	65.2
3	97.5	91.6	60.6
4	97.6	91.8	56.5
5	97.7	87.1	59.8
6	96.7	92	61.7
7	96.3	91.6	64.3
8	97.5	91.5	60.5
Mean	97.312	83.675	61.362
Standard Deviation	0.52	13.54	2.72

Chemical Content

The chemical contents of the carbon produced were investigated by Raman spectroscopy, Fourier-transform infrared spectroscopy (FTIR), and Brunaur-Emmett-Teller (BET). Raman spectroscopy has been largely used in characterizing solid materials in general and carbon materials in particular. Raman spectra appear in two frequency domains, 1340–1650 cm^{-1}, corresponding to G and D bands characteristic to carbon compounds, and 2600–3400 cm^{-1}, corresponding to G and D bands overtones. Their positions and widths depend on the material carbonization degree and the disorder (porosity, crystallite size distribution, concentration of amorphous component) [35]. The Raman test in this study generates a graph with the intensity of D band and G band values on the range of the frequency (Raman shift) from 200–3000 cm^{-1}.

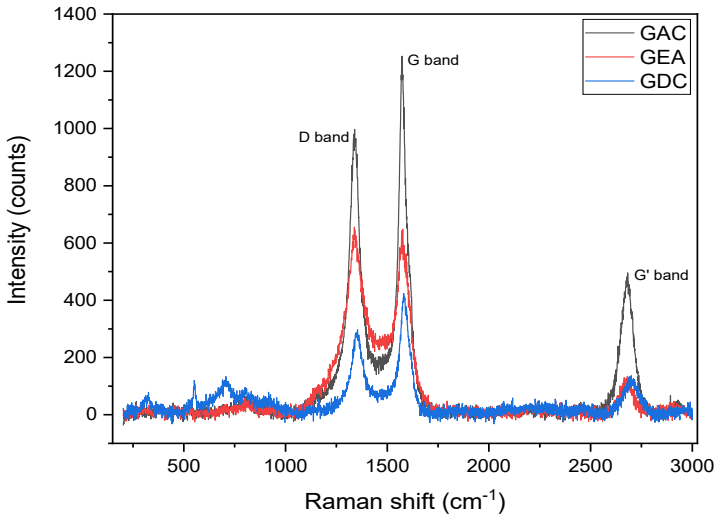

Figure 7. Graphic of Raman test

The peaks of the D band, G band, and G' band are detected in all samples, as shown in Figure 7. The D-band (defect band) is related to the disorder induced in the carbon material, and the G band is the optical phonon of carbon atoms moving around in phase opposition [36]. The G band intensity of carbon powder at GAC and GDC samples is higher than the D band intensity. On the contrary, in the GEA sample, the G band intensity is lower than the D band, as shown in Table 2. The intensity ratio between D and G bands (I_D/I_G) is often used to evaluate the disorder in carbon materials or estimate the amounts of defects in the graphitic walls [37]. Based on the ratio I_D/I_G band shown in Table 2, carbon material from GEA precursor has higher disorder properties than carbon material from GAC and GDC precursors. In advance, carbon material from the GAC precursor has low disorder properties because it has a higher I_D/I_G value than the carbon material from the GDC precursor. Disorder properties are the characteristics of a material that show its degree of amorphousness and defects [38].

Table 2. Shows Intensity of D band and G band from Raman test

Sample	I_D	I_G	I_D/I_G
GAC	996.94	1252.81	0.79
GEA	655.58	648.91	1.01
GDC	296.99	411.77	0.72

FTIR spectroscopy is an analytical method used to characterize the bonding structure of atoms based on the interaction of infrared radiation with matter. It measures the frequencies of the radiation at which the substance absorbs and leads to the production of vibrations in molecules [39]. In this study, FTIR spectroscopy is performed on the infrared intensity as a function of wavenumber in the Mid-Infrared spectral range, i.e., 400–4000 cm^{-1}, as shown in Figure 8.

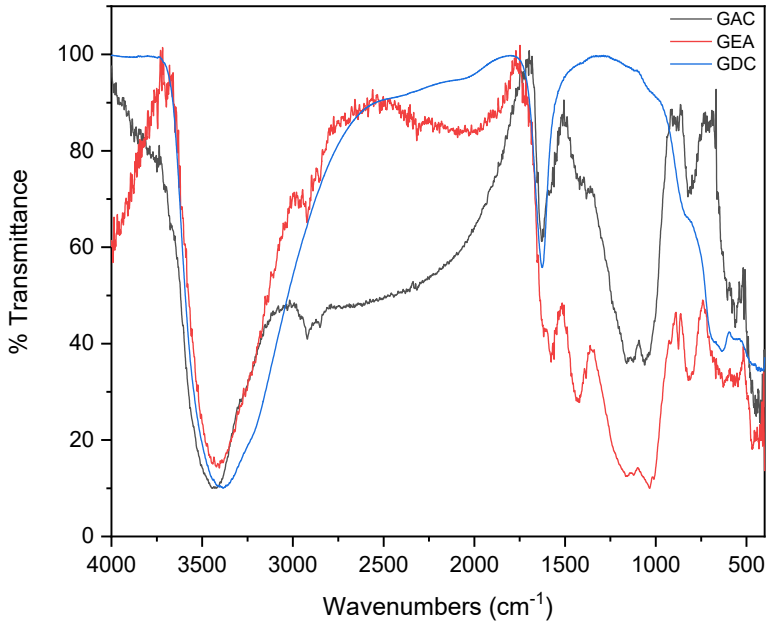

Figure 8. Graph of FTIR test result

According to the FTIR spectroscopy results graph in Figure 8, all specimens showed a decreased transmittance percentage in the wavenumber range of 3000–3450 cm^{-1}. This indicates the formation of the O–H stretching caused by the absorption process on the material when synthesized in the atmosphere [40]. The functional groups that occurred in each sample can be seen in Table 3.

Table 3. Shows functional group analysis on the sample

Sample	Wavenumber (cm^{-1})	Ref. Wavenumber (cm^{-1})	Functional group
GAC	1159.70	1160	C–O stretching [39]
	1629.07	1670–1600	N–H bending [41]
	2920.49	3000–2800	C–H stretching [39]
	3444.89	3450–3350	O–H stretching [40]
GEA	1033.43	1036	C–N stretching [40]
	1560.44	1560	C–C stretching [42]
	2921.91	3000–2800	C–H stretching [39]
	3405.39	3450–3350	O–H stretching [40]
GDC	636.72	633	C–Cl stretching [40]
	1625.11	1670–1600	N–H bending [41]
	3383.77	3450–3350	O–H stretching [40]

Carbon material from the GDC precursor showed the formation of the C–Cl stretching at wavenumber 636.72 cm^{-1}. It was formed due to the usage of a dichloromethane solvent containing chlorine that generates C–Cl [40]. The functional groups of C–N, N–O, and N–H formed on the sample because, in this study, nitrogen was used as a carrier gas. With this setup, the functional groups of aliphatic nitro compounds may be formed in all samples as a result of the nitrogen reaction with hydrogen and oxygen in the atmosphere.

BET is a test to determine the surface area, pore volume, and physical properties of the carbon material. The BET test is performed by exposing a solid material to a gas or vapor under different conditions and measuring the increase in weight or volume of the sample. Nitrogen gas is generally used as a gas exposed to solid material for this test [43]. The BET surface area and pore volume of the carbon material from precursor GAC and GEA with different concentrations are shown in Table 4. Precursor GDC was not included in this test due to the chlorine content, which may be harmful, and also its low carbon yield.

Table 4. Result of the BET test

Sample	Ratio gondorukem:solvent	BET Surface Area (m^2/g)	Pore Volume (cm^3/g)
GAC	1:4	15.70 ± 0.19	0.03
	1:8	10.71 ± 0.11	0.02
	1:16	14.77 ± 0.17	0.03
GEA	1:4	27.80 ± 0.23	0.05
	1:8	58.71 ± 0.36	0.11
	1:16	48.31 ± 0.32	0.06

According to Table 4, the carbon material from the GEA precursor has a greater BET surface area value of 58.71 m^2/g at GEA 1:8 than the carbon material from the GAC precursor. However, the pore volume generated on the carbon material from the GAC precursor has a lower value, reaching 0.02 cm^3/g in the GAC precursor with a 1:8 ratio. The larger surface area value indicates that the material carbon has a smaller particle size. When the pore volume decreases, the material becomes denser [44]. An efficient carbon material as a filter material in the mask layer is one with a large surface area and a large number of pores that serve as an absorbent container for filtered material [45].

CONCLUSION

Carbon microstructures have been successfully synthesized from pine resin (gondorukem) using various solvents, acetone (GAC), ethyl acetate (GEA), and dichloromethane (GDC). The field emission scanning electron microscopy (FE-SEM) investigation indicated the presence of nanoparticles. Carbon material from the GAC precursor has an average size of 283.58 nm and the highest carbon content, which reached an average of 97.312 %wt compared to the GEA and GDC samples, which contain carbon contents of 83.675 %wt and 61.362 %wt. It also had the lowest disorder properties in the Raman spectroscopy test, with the value of I_D/I_G reaching 0.795764, and formed several functional groups of carbon, i.e., C–H stretching at wavenumber 2920.49 cm^{-1}, N–H bending at wavenumber 1629.07 cm^{-1}, and C–O stretching at wavenumber 1159.70 cm^{-1} based on the Fourier-transform infrared spectroscopy (FTIR) test. The carbon material from the GEA precursor with a ratio of 1:8 has the highest value of Brunaur-Emmett-Teller (BET) surface area and pore volume, reaching 58.71 ± 0.36 m^2/g and 0.11 cm^3/g, respectively. Therefore, based on carbon content, disorder properties, and functional group stabilization, the carbon material from the GAC precursor provides the ideal characteristics to be used as a filter material in medical masks. Meanwhile, based on BET testing, the carbon materials from GEA precursor with a ratio of 1:8 have the ideal material morphological properties to be used as a filter on a medical mask.

ACKNOWLEDGEMENT

We would like to thank the Bio-physic Graduate School of IPB University and High Resistance Material Group, Research Center for Advanced Material, Research Organization of Nanotechnology and Material for the facilities and funding that support the research process. This research is also partly funded by the Degree by Research scheme of BRIN. Characterization and analyses were supported by ELSA-BRIN.

REFERENCES

[1] M. Yang, C. Fang, J. Su, Y. Cheng, Q. Zhang, and M. Liu. "Synthesis mechanism of carbon microsphere from waste office paper via hydrothermal method." *BioReources*, vol. 17, no. 4, pp. 5568–5577, 2022.

[2] C. Li, J. Yang, L. Zhang, S. Li, Y. Yuan, X. Xiao, X. Fan, and C. Song. "Carbon-based membrane materials and applications in water and wastewater treatment: A review." *Environ. Chem. Lett.*, vol. 19, pp. 1457–1475, 2020.

[3] S. Jiang, Q. Chen, J. Lin, G. Liao, T. Shi, and L. Qian. "Thermal stress-induced fabrication of carbon micro/nanostructures and the application in high-performance enzyme-free glucose sensors." *Sens. Actuators B. Chem.*, vol. 345, p. 130364, 2021.

[4] P. Yu, W. Tang, F. -F. Wu, C. Zhang, H. -Y. Luo, H. Liu, and Z. -G. Wang. "Recent progress in plant-derived hard carbon anode materials for sodium-ion batteries: A review." *Rare Met.*, vol. 39, no. 9, pp. 1019–1033, 2020.

[5] B. A. Alshammari, A. N. Wilkinson, B. M. Alotaibi, and M. F. Alotibi. "Influence of carbon micro-and nano-fillers on the viscoelastic properties of polyethylene terephthalate." *Polymers (Basel)*, vol. 14, no. 12, 2022.

[6] E. Antolini. "Carbon supports for low-temperature fuel cell catalysts." *Applied Catalysis B: Environmental*, vol. 88, no. 1–2. pp. 1–24, 2009.

[7] U. Kamran, Y. J. Heo, J. W. Lee, and S. J. Park. "Functionalized carbon materials for electronic devices: A review," *Micromachines (Basel)*, vol. 10, no. 4, pp. 1–26, 2019.

[8] J. Leng, Z. Wang, J. Wang, H. H. Wu, G. Yan, X. Li, H. Guo, Y. Liu, Q. Zhang, and Z. Guo. "Advances in nanostructures fabricated via spray pyrolysis and their applications in energy storage and conversion." *Chem. Soc. Rev.*, vol. 48, no. 11, pp. 3015–3072, 2019.

[9] N. Saito, Y. Usui, K. Aoki, N. Narita, M. Shimizu, K. Hara, N. Ogiwara, K. Nakamura, N. Ishigaki, H. Kato, S. Taruta, and M. Endo. "Carbon nanotubes: Biomaterial applications." *Chem. Soc. Rev*., vol. 38, no. 7, pp. 1897–1903, 2009.
[10] S. Y. Lim, W. Shen, and Z. Gao. "Carbon quantum dots and their applications." *Chem. Soc. Rev.*, vol. 44, no. 1, pp. 362–381, 2015.
[11] A. Sharma and J. Das. "Small molecules derived carbon dots: Synthesis and applications in sensing, catalysis, imaging, and biomedicine." *Journal of Nanobiotechnology*, vol. 17, no. 92, 2019.
[12] J. Li, Z. Xu, L. Yu, and L. Zhang. "Preparation of hundred-micron carbon spheres using solvent extraction in a simple microchannel device." *Microporous and Mesoporous Materials*, vol. 343, p. 112186, 2022.
[13] Q. Wang, F. Cao, Q. Chen, and C. Chen. "Preparation of carbon micro-spheres by hydrothermal treatment of methylcellulose sol." *Material Letters*, vol. 59, no. 28, pp. 3738–3741, 2005.
[14] S. Ratchahat, N. Viriya-empikul, K. Faungnawakij, T. Charinpanitkul, A. Soottitantawat. "Synthesis of carbon microspheres from starch by hydrothermal process." Sci. J. UBU, vol.1, no. 2, pp. 40-45, 2010.
[15] K. G. Latham, I. Kozyatnyk, J. Figueira, M. Carlborg, E. Rosenbaum, and S. Jansson, "Self-generation of low ash carbon microspheres from the hydrothermal supernatant of anaerobic digestate: Formation insights and supercapacitor performance." *Chemical Engineering Journal Advances*, vol. 6, p. 100097, 2021.
[16] D. L. Sivadas, R. Narasimman, R. Rajeev, K. Prabhakaran, and K. N. Ninan. "Solvothermal synthesis of microporous superhydrophobic carbon with tunable morphology from natural cotton for carbon dioxide and organic solvent removal applications." *J. Mater. Chem. A*, vol. 3, no. 31, pp. 16213–16221, 2015.
[17] A. Bazargan, Y. Yan, C. W. Hui, and G. McKay. "A review: Synthesis of carbon-based nano and micro materials by high temperature and high pressure." *Industrial and Engineering Chemistry Research*, vol. 52, no. 36. pp. 12689–12702, 2013.
[18] J. K. Kim, Y. Yoo, and Y. C. Kang. "Scalable green synthesis of hierarchically porous carbon microspheres by spray pyrolysis for high-performance supercapacitors." *Chemical Engineering Journal*, vol. 382, p. 122805, 2020.
[19] Y. Wang and A. Hu. "Carbon quantum dots: Synthesis, properties and applications." *J. Mater. Chem. C*, vol. 2, pp. 6921–6939, 2014.
[20] L. Ndlwana, N. Raleie, K. M. Dimpe, H. F. Ogutu, E. O. Oseghe, M. M. Motsa, T. A. M. Msagati, and B. B. Mamba. "Sustainable hydrothermal and solvothermal synthesis of advanced carbon materials in multidimensional applications: A review." *Materials*, vol. 14, no. 17, 2021.
[21] S. E. Skrabalak, "Ultrasound-assisted synthesis of carbon materials." *Physical Chemistry Chemical Physics*, vol. 11, no. 25, pp. 4930–4942, 2009.
[22] D. S. Jung, S. Bin Park, and Y. C. Kang. "Design of particles by spray pyrolysis and recent progress in its application." *Korean Journal of Chemical Engineering*, vol. 27, no. 6, pp. 1621–1645, 2010.
[23] M. I. Ionescu, Y. Zhang, R. Li, X. Sun, H. Abou-Rachid, and L. S. Lussier, "Hydrogen-free spray pyrolysis chemical vapor deposition method for the carbon nanotube growth: Parametric studies." *Appl. Surf. Sci.*, vol. 257, no. 15, pp. 6843–6849, 2011.
[24] M. U. Zahid, E. Pervaiz, A. Hussain, M. I. Shahzad, and M. B. K. Niazi. "Synthesis of carbon nanomaterials from different pyrolysis techniques: A review." *Mater. Res. Express*, vol. 5, no. 5, 2018.
[25] A. Darabont, P. Nemes–Incze, K. Kertesz, L. Tapaszto, A. A. Koos, Z. Osvath, Zs. Sarkozi, Z. Vertesy, Z. E. Horvath, and L. P. Biro. "Synthesis of carbon nanotubes by spray pyrolysis and their investigation by electron microscopy." *Journal of Optoelectronics and Advanced Materials*, vol. 7, no. 2, pp. 631–636, 2005.
[26] J. Lara-Romero, T. Ocampo-Macias, R. Martínez-Suarez, R. Rangel-Segura, J. López-Tinoco, F. Paraguay-Delgado, G. Alonso-Nuñez, S. Jiménez-Sandoval, and F. Chiñas-Castillo. "Parametric study of the synthesis of carbon nanotubes by spray pyrolysis of a biorenewable feedstock: α-pinene." *ACS Sustain. Chem. Eng.*, vol. 5, no. 5, pp. 3890–3896, 2017.
[27] A. V. Melezhik, M. A. Smykov, E. Yu. Filatova, A. V. Shuklinov, R. A. Stolyarov, I. S. Larionova, and A. G. Tkachov. "Synthesis of carbon nanotubes from acetone." *Theoretical Foundations of Chemical Engineering*, vol. 47, no. 4, pp. 435–443, Jul. 2013.
[28] Z. Xue, Y. Shen, P. Li, Y. Zhang, Y. Zeng, and S. Zhu. "Controllable synthesis of carbon nanotubes via autothermal reforming of ethyl acetate." *Mater. Des.*, vol. 141, pp. 150–158, 2018.
[29] A. Li, J. Wang, K. Zhang, W. Fu, L. Cheng, Dr. M. Zhang. "Preparation of porous carbon from dichloromethane and p-phenylenediamine with short KOH activation depth." Chem. Electro Chem., vol. 9, no. 10, p. e202200190, 2022.
[30] R. A. Afre, T. Soga, T. Jibo, M. Kumar, Y. Ando, M. Sharon, P. R. Somani, M. Umeno. "Carbon nanotubes by spray pyrolysis of turpentine oil at different temperatures and their studies," *Microporous and Mesoporous Materials*, vol. 96, no. 1–3, pp. 184–190, 2006.
[31] Perum Perhutani, "Laporan Tahunan Perum Perhutani Tahun 2018," Jakarta, Indonesia, 2018.
[32] M. de la Garza, I. López, and I. Gómez. "In situ synthesis and deposition of gold nanoparticles with different morphologies on glass and ITO substrate by ultrasonic spray pyrolysis." *Advances in Materials Science and Engineering*, vol. 2013, 2013.
[33] E. Brimas, R. Skaudžius, G. Brimas, A. Selskis, R. Ramanauskas, and A. Kareiva. "Three different techniques to reconstruct 3D view of SEM images by using only free available software." CHEMIJA, vol. 33, no. 1, pp. 7–11, 2022.

[34] J. Jeevanandam, A. Barhoum, Y. S. Chan, A. Dufresne, and M. K. Danquah. "Review on nanoparticles and nanostructured materials: History, sources, toxicity and regulations." *Beilstein J. of Nanotechnol.*, vol. 9, no. 1, pp. 1050–1074, 2018.
[35] C. Sisu, R. Iordanescu, V. Stanciu, I. Stefanescu, A. M. Vlaicu, and V. V. Grecu. "Raman spectroscopy studies of some carbon molecular sieves." *Dig. J. Nanomater. Biostruct.*, vol. 11, no. 2, pp. 435–442, 2016.
[36] M. S. Dresselhaus, A. Jorio, A. G. Souza Filho, and R. Saito. "Defect characterization in graphene and carbon nanotubes using Raman spectroscopy." *Phil. Trans. R. Soc. A*, vol. 368, no. 1932, pp. 5355–5377, 2010.
[37] S. Osswald and Y. Gogotsi. "In Situ Raman Spectroscopy of Oxidation of Carbon Nanomaterials," in *Raman Spectroscopy for Nanomaterials Characterization*, Springer Nature, 2012, pp. 291–351.
[38] P. Puech, M. Kandara, G. Paredes, L. Moulin, E. Wiss-Hortala, A. Kundu, N. Ratel-Ramond, J. -M. Plewa, R. Pellenq, and M. Monthioux. "Analyzing the raman spectra of graphenic carbon materials from kerogens to nanotubes: What type of information can be extracted from defect bands?" *Journal of Carbon Research*, vol. 5, no. 4, p. 69, 2019.
[39] V. Ţucureanu, A. Matei, and A. M. Avram. "FTIR spectroscopy for carbon family study." *Crit. Rev. Anal. Chem.*, vol. 46, no. 6, pp. 502–520, 2016.
[40] J. Zhuang, M. Li, Y. Pu, A. J. Ragauskas, and C. G. Yoo. "Observation of potential contaminants in processed biomass using fourier transform infrared spectroscopy." *Appl. Sci*, vol. 10, no. 12, pp. 1–13, 2020.
[41] J. Sukprasert, K. Thumanu, I. Phung-on, C. Jirarungsatean, L. E. Erickson, P. Tuitemwong, and K. Tuitemwong. "Synchrotron FTIR light reveals signal changes of biofunctionalized magnetic nanoparticle attachment on salmonella sp.," *J. Nanomater.*, vol. 2020, 2020.
[42] D. S. Volkov, P. K. Krivoshein, and M. A. Proskurnin. "Detonation nanodiamonds: A comparison study by photoacoustic, diffuse reflectance, and attenuated total reflection FTIR spectroscopies." *Nanomaterials*, vol. 10, no. 12, pp. 1–37, 2020.
[43] G. Sdanghi, R. L. S. Canevesi, A. Celzard, M. Thommes, and V. Fierro. "Characterization of carbon materials for hydrogen storage and compression." *C—Journal of Carbon Research*, vol. 6, no. 3, p. 46, 2020.
[44] M. Maryam, A. B. Suriani, M. S. Shamsudin, and M. Rusop, "BET analysis on carbon nanotubes: Comparison between single and double stage thermal CVD method." *Adv. Mat. Res.*, vol. 626, pp. 289–293, 2013.
[45] W. K. Essa, S. A. Yasin, I. A. Saeed, and G. A. M. Ali. "Nanofiber-based face masks and respirators as COVID-19 protection : A review." Membranes, vol. 11, no. 4, p. 250, 2021.